JACS
JOURNAL OF THE AMERICAN CHEMICAL SOCIETY

Subscriber access provided by ISTANBUL TEKNIK UNIV

Article

Self-Sorting Chiral Subcomponent Rearrangement During Crystallization

Marie Hutin, Christopher J. Cramer, Laura Gagliardi, Abdul Rehaman Moughal Shahi, Grald Bernardinelli, Radovan Cerny, and Jonathan R. Nitschke

J. Am. Chem. Soc., **2007**, 129 (28), 8774-8780• DOI: 10.1021/ja070320j • Publication Date (Web): 26 June 2007

Downloaded from http://pubs.acs.org on February 16, 2009

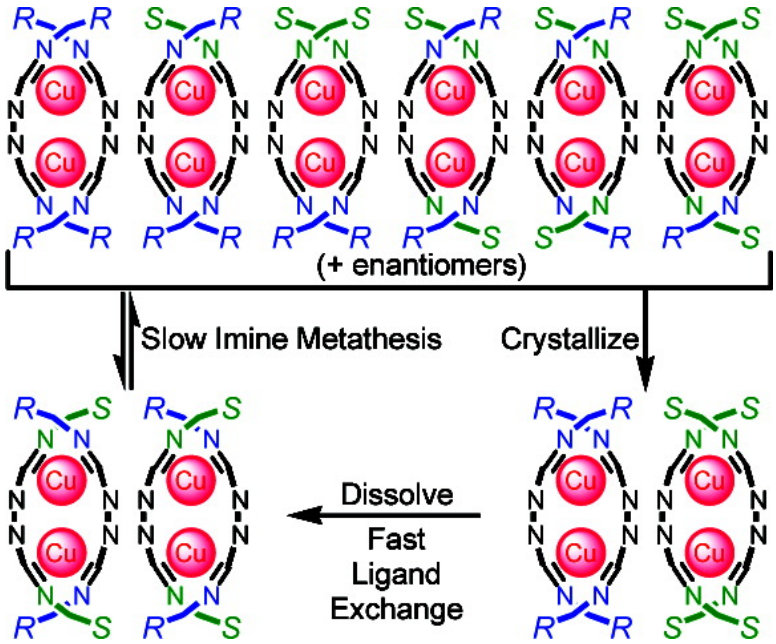

More About This Article

Additional resources and features associated with this article are available within the HTML version:

- Supporting Information
- Links to the 16 articles that cite this article, as of the time of this article download
- Access to high resolution figures
- Links to articles and content related to this article
- Copyright permission to reproduce figures and/or text from this article

View the Full Text HTML

ACS Publications
High quality. High impact.

Journal of the American Chemical Society is published by the American Chemical Society. 1155 Sixteenth Street N.W., Washington, DC 20036

J|A|C|S
ARTICLES
Published on Web 06/26/2007

Self-Sorting Chiral Subcomponent Rearrangement During Crystallization

Marie Hutin,[†] Christopher J. Cramer,[‡] Laura Gagliardi,[§] Abdul Rehaman Moughal Shahi,[§] Gérald Bernardinelli,[⊥] Radovan Cerny,[⊥] and Jonathan R. Nitschke*,[†]

Contribution from the Department of Organic Chemistry, University of Geneva, 30 Quai Ernest Ansermet, 1211 Genève 4, Switzerland, Department of Chemistry and Supercomputing Institute, University of Minnesota, 207 Pleasant Street SE, Minneapolis, Minnesota 55455-0431, Department of Physical Chemistry, University of Geneva, 30 Quai Ernest Ansermet, 1211 Genève 4, Switzerland, and Laboratory of X-Ray Crystallography, University of Geneva, 24 quai Ernest Ansermet, 1211 Genève 4, Switzerland

Received January 21, 2007; E-mail: Jonathan.Nitschke@chiorg.unige.ch

Abstract: The incorporation of enantiopure 1-amino-2,3-propanediol as a subcomponent into a dicopper double helicate resulted in perfect chiral induction of the helicate's twist. DFT calculations allowed the determination of the helicity of the complex in solution. The same helical induction, in which *S* amines induced a Λ helical twist, was observed in the solid state by X-ray crystallography. Electronic structure calculations also revealed that the unusual deep green color of this class of complexes was due to a metal-to-ligand charge transfer excitation, in which the excited state possesses a valence delocalized Cu_2^{3+} core. The use of a racemic amine subcomponent resulted in the formation of a dynamic library of six diastereomeric pairs of enantiomers. Surprisingly, this library converted into a single pair of enantiomers during crystallization. We were able to observe this process reverse upon redissolution, as initial ligand exchange was followed by covalent imine metathesis.

Introduction

Starting with Pasteur's original demonstration of the spontaneous resolution of tartrate salts during crystallization,[1] the expression of chiral information during the process of crystallization has provoked much interest and led to a great deal of fundamental understanding. A binary mixture of enantiomers may crystallize in three fundamentally different ways. First, the most common crystallization mode of a racemate is the formation of a homogeneous crystal structure, commonly known as a racemic compound. Racemic compounds very frequently crystallize in centrosymmetric space groups, but cases of such compounds forming noncentrosymmetric, and even chiral, crystal structures are known.[2] Theories have been developed by Collet and co-workers,[3,4] Schipper and co-workers,[5−7] and Dunitz and co-workers[8] as to why racemic compounds tend to form during the crystallization of racemates; both thermodynamic and kinetic factors appear to work in their favor.[9] Second, as in the case of sodium ammonium tartrate tetrahydrate,[1] each enantiomer may crystallize separately, forming two sets of distinct, enantiomorphic crystals. The space group of a chiral crystal must contain only translations and rotations as symmetry operations, which limits it to one of only 65 of the 230 space groups. Third, the rarest and least-studied case is the formation of a solid solution of a mixture of the two enantiomers. These solid solutions are now known as pseudoracemates,[10] a term originally coined by Kipping and Pope[11] to describe crystals twinned by inversion. The crystal structures of these solid solutions are disordered in a way that some sites are occupied by a molecule of either chirality. Pseudoracemates tend to be favored in cases in which intermolecular crystal packing discriminates poorly between the enantiomers; Ward and Custelcean have recently described a system in which this situation may be favored by inclusion of chiral substrates within a hydrogen-bonded framework, which can isolate the substrates from each other.[9]

In the present work, we describe a system complementing and extending prior studies of crystallization from racemic mixtures. The system presented herein consists of a dicopper double helicate that contains four chiral amine subcomponents.[12] When an enantiopure amine was employed as a subcomponent, only one product diastereomer was observed. DFT calculations allowed us to determine the direction of helicate twist induced

[†] Department of Organic Chemistry, University of Geneva.
[‡] University of Minnesota.
[§] Department of Physical Chemistry, University of Geneva.
[⊥] Laboratory of X-Ray Crystallography, University of Geneva.

(1) Pasteur, L. *Ann. Chim. Phys.* **1848**, *24*, 442−459.
(2) Flack, H. D. *Helv. Chim. Acta* **2003**, *86*, 905−921.
(3) Collet, A. *Angew. Chem., Int. Ed.* **1998**, *37*, 3239−3241.
(4) Collet, A.; Brienne, M. J.; Jacques, J. *Chem. Rev.* **1980**, *80*, 215−230.
(5) Schipper, P. E. *J. Am. Chem. Soc.* **1978**, *100*, 1079−1084.
(6) Schipper, P. E.; Harrowell, P. R. *J. Am. Chem. Soc.* **1983**, *105*, 723−730.
(7) Craig, D. P.; Schipper, P. E. *Chem. Phys. Lett.* **1974**, *25*, 476−479.
(8) Brock, C. P.; Schweizer, W. B.; Dunitz, J. D. *J. Am. Chem. Soc.* **1991**, *113*, 9811−9820.
(9) Custelcean, R.; Ward, M. D. *Cryst. Growth Des.* **2005**, *5*, 2277−2287.
(10) Jacques, J.; Collet, A.; Wilen, S. H. *Enantiomers, Racemates and Resolutions;* Wiley & Sons: New York, 1981.
(11) Kipping, F. S.; Pope, W. J. *J. Chem. Soc.* **1897**, *71*, 989−1001.
(12) Nitschke, J. R. *Acc. Chem. Res.* **2007**, *40*, 103−112.

10.1021/ja070320j CCC: $37.00 **© 2007 American Chemical Society**

Scheme 1. Synthesis of 4*S* Helicate **1**, the Helical Λ-Chirality of Which was Assigned from Its CD Spectrum

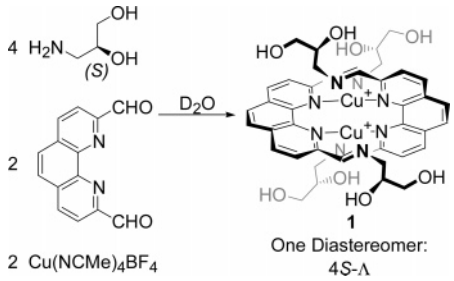

by the amines' chirality, in addition to explaining the nature of the electronic transitions responsible for the unusual dark green color of this class of helicates.[13]

When the racemate of the same chiral amine was employed, the system gained considerable complexity. Since either enantiomer may be incorporated at each equivalent location, a statistical mixture of diastereomers would be expected, since the reaction did not appear to be inherently diastereoselective. Upon crystallization, the various diastereomeric pairs of enantiomers might independently form different enantiopure or racemic crystals, or all might crystallize together to form a solid−solution crystal in which the *R* and *S* amine residues are distributed at random.

Since the chiral amine subcomponents are capable of exchange, however, the set of diastereomers represents a dynamic combinatorial library,[14−16] or interconverting mixture, of structures. Another possibility thus exists during crystallization: If one pair of enantiomers was less soluble than the other diastereomers, the preferential crystallization of this pair could result in the elimination of all others from the dynamic library. Exchange of the amine residues allowed the least soluble enantiomers to be regenerated as they were drained from the mixture during crystallization, sorting the library into a single pair of least soluble enantiomers. This process resulted in the formation of racemic crystals, which was unsurprising in that this is the most common outcome when a mixture of enantiomers is crystallized.[9] It is somewhat more surprising, however, to have observed the clean conversion of a complex mixture of *diastereomers* into racemic crystals.

Results and Discussion

As shown in Scheme 1, the reaction of 2,9-diformyl-1,10-phenanthroline and chiral 1-amino-2,3-propanediol with copper(I) tetrafluoroborate in water gave dicopper double helicate **1** as the unique product.

As was observed in a monocopper(I) case,[17] the incorporation of enantiopure amine residues resulted in the transfer of chiral information from the fixed carbon stereocenters to the stereochemically labile helical core. When enantiopure (*S*) amine was employed as a subcomponent, only one set of NMR signals was observed for the product helicate **1**, even upon cooling to 193 K in CD_3OD. This indicated the presence of only a single product diastereomer.

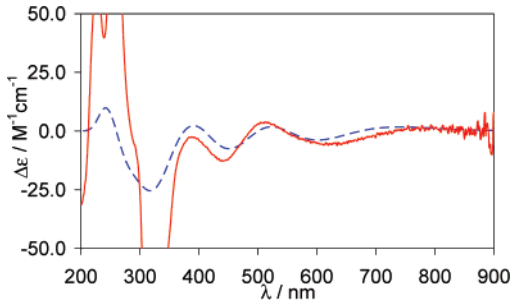

Figure 1. Experimental (solid red) CD spectrum for **1** in methanol and simulated (dashed blue) CD spectrum for Λ-**1a**, which contains iminomethanes in place of the iminopropanediol residues of **1**.

The circular dichroism (CD) spectrum of **1** (Figure 1) was also consistent with the presence of only a single diastereomer: Strong Cotton effects were noted ($\Delta\epsilon_{max} = -198.2$ M^{-1} cm^{-1} at 315 nm, 293 K).

We know of no straightforward way to assign the helical chirality of a complex such as **1** based upon direct interpretation of the spectrum, as is possible in certain mononuclear cases.[17−20] Electronic structure calculations were therefore undertaken to assign and understand this spectrum and to answer broader questions as to the nature of the electronic excitations of dicopper helicates of this type. The metal-to-ligand charge transfer (MLCT) transitions of copper(I) complexes have long been subjects of interest in the context of solar energy conversion.[21−25] The deep green coloration of dicopper helicates such as **1**, first noted by Ziessel et al.,[13] is unusual for a Cu^I complex and suggestive of an excited state of atypical electronic structure.

For computational purposes, a slightly simplified model for **1** was constructed in which each iminopropanediol group was replaced by an iminomethane group; we refer to this construct as **1a**. The geometry of **1a** was optimized at the density functional (DFT) level of theory using the generalized gradient approximation (GGA) functional BP86[26,27] with a polarized split valence basis set.[28−30] Including the effects of aqueous solvation with the COSMO continuum solvation model[31] had little effect on the optimized geometry; the Cu−Cu distance decreased from 2.68 to 2.67 Å (experimental: 2.74 Å; see below) and the various Cu−N distances also shortened by 0.01 Å or less. Computation of analytic vibrational frequencies verified the D_2 structure as a minimum.

(13) Ziessel, R.; Harriman, A.; Suffert, J.; Youinou, M.-T.; De Cian, A.; Fischer, J. *Angew. Chem., Int. Ed.* **1997**, *36*, 2509−2511.
(14) Corbett, P. T.; Leclaire, J.; Vial, L.; West, K. R.; Wietor, J. L.; Sanders, J. K. M.; Otto, S. *Chem. Rev.* **2006**, *106*, 3652−3711.
(15) Rowan, S. J.; Cantrill, S. J.; Cousins, G. R. L.; Sanders, J. K. M.; Stoddart, J. F. *Angew. Chem., Int. Ed.* **2002**, *41*, 898−952.
(16) Brooker, S.; Hay, S. J.; Plieger, P. G. *Angew. Chem., Int. Ed.* **2000**, *39*, 1968−1970.
(17) Hutin, M.; Nitschke, J. R. *Chem. Commun.* **2006**, 1724−1726.
(18) Amendola, V.; Fabbrizzi, L.; Mangano, C.; Pallavicini, P.; Roboli, E.; Zema, M. *Inorg. Chem.* **2000**, *39*, 5803−5806.
(19) Woods, C. R.; Benaglia, M.; Cozzi, F.; Siegel, J. S. *Angew. Chem., Int. Ed.* **1996**, *35*, 1830−1833.
(20) Ziegler, M.; von Zelewsky, A. *Coord. Chem. Rev.* **1998**, *177*, 257−300.
(21) Dietrich-Buchecker, C. O.; Marnot, P. A.; Sauvage, J. P.; Kirchhoff, J. R.; McMillin, D. R. *Chem. Commun.* **1983**, 513−515.
(22) Kalsani, V.; Schmittel, M.; Listorti, A.; Accorsi, G.; Armaroli, N. *Inorg. Chem.* **2006**, *45*, 2061−2067.
(23) Williams, R. M.; De Cola, L.; Hartl, F.; Lagref, J. J.; Planeix, J. M.; De Cian, A.; Hosseini, M. W. *Coord. Chem. Rev.* **2002**, *230*, 253−261.
(24) Sakaki, S.; Kuroki, T.; Hamada, T. *J. Chem. Soc., Dalton Trans.* **2002**, 840−842.
(25) Felder, D.; Nierengarten, J. F.; Barigelletti, F.; Ventura, B.; Armaroli, N. *J. Am. Chem. Soc.* **2001**, *123*, 6291−6299.
(26) Becke, A. D. *Phys. Rev. A* **1988**, *38*, 3098−3100.
(27) Perdew, J. P. *Phys. Rev. B* **1986**, *33*, 8822−8824.
(28) Schäfer, A.; Horn, H.; Ahlrichs, R. *J. Chem. Phys.* **1992**, *97*, 2571−2577.
(29) Ahlrichs, R.; Bär, M.; Häser, M. *Chem. Phys. Lett.* **1989**, *162*, 165.
(30) Haser, M.; Ahlrichs, R. *J. Comput. Chem.* **1989**, *10*, 104−111.
(31) Schäfer, A.; Klamt, A.; Sattel, D.; Lohrenz, J. C. W.; Eckert, F. *Phys. Chem. Chem. Phys.* **2000**, *2*, 2187−2193.

Table 1. Vertical Excitation Energies (nm), Oscillator Strengths (unitless), and Transition Characters Predicted for **1a**

excitation	B3LYP[a]	BP86
HOMO → LUMO+2	730 (0.028)	1059 (0.004)
HOMO → LUMO	726 (0.000)	1129 (0.000)
HOMO → LUMO+1	722 (0.014)	1176 (0.003)
HOMO−1 → LUMO+2	614 (0.003)	834 (0.011)
HOMO−1 → LUMO	609 (0.000)	909 (0.000)
HOMO−1 → LUMO+1	594 (0.014)	837 (0.033)

[a] With 6-31G(d) basis set[36] on H, C, and N and a Stuttgart pseudopotential[37] on Cu using Gaussian 03.[38]

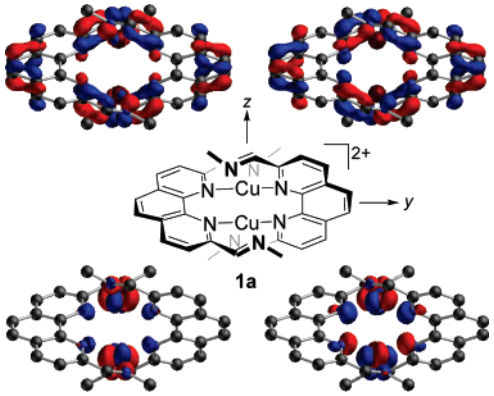

Figure 2. Diagram of **1a** (center) viewed down the *x* twofold axis of symmetry, showing its *y* and *z* axes. The HOMO−1 (lower left), HOMO (lower right), LUMO (upper left), and LUMO+1 (upper right) orbitals of **1a** (at the 0.04 au contour level) are shown. Hydrogen atoms have been removed for clarity.

Vertical electronic excitation energies were computed at the time-dependent (TD) DFT level[32] for the aqueous geometry using both the BP86 functional and the hybrid GGA B3LYP[26,33−35] functional (Table 1). Both levels predict three very long wavelength MLCT excitations having relatively similar energies.

These transitions are well described as being one-electron excitations from the highest occupied molecular orbital (HOMO) to the lowest unoccupied molecular orbital (LUMO), LUMO+1, and LUMO+2. The HOMO is dominated by a nonbonding combination of the d_{xy} orbital on one copper and the $d_{x^2-y^2}$ orbital on the other (the *y* and *z* axes of symmetry are shown in Figure 2). The first two virtual orbitals are nearly degenerate positive and negative linear combinations of equivalent π^* ligand orbitals (Figure 2), and the LUMO+2 is another low-energy π^* orbital delocalized over the ligands. An additional three excitations are predicted to occur at somewhat higher energy from the HOMO−1 into each of these orbitals. The HOMO−1 is essentially identical to the HOMO, except that weak contributions from the nitrogen lone pairs in this orbital are in phase with one another while in the HOMO they are out of phase, raising the energy of the latter slightly. While the B3LYP level provides excitation energies in good agreement with experiment, the BP86 predictions are substantially too low in energy, which is consistent with the tendency of pure GGA functionals to underestimate the energies of MLCT transitions.[39]

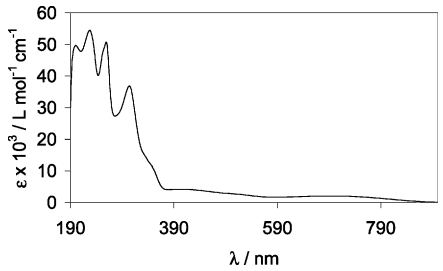

Figure 3. UV−vis spectrum of **1** in methanol.

The unusual dark green color of **1** and its congeners[13,40,41] is thus a consequence of the delocalization of the HOMO and the HOMO−1 across both copper(I) ions. The energies of MLCT excitations from these two orbitals into the ligand-based LUMO manifold are lowered by the delocalization of the increased metal charge over both Cu atoms. A transient mixed valence[42] $Cu^{1.5+}$-$Cu^{1.5+}$ state is thus generated, similar to the mixed valence dicopper helicate recently described by Jeffery et al.[43] A very broad absorption feature is observed centered at 688 nm, a much longer wavelength than that for mononuclear copper(I) tetraimine complexes (ca. 475 nm).[17] The spectral minimum at 565 nm between the MLCT excitations and the higher-energy $\pi \rightarrow \pi^*$ absorptions thus defines the green color of **1**. The UV−vis spectrum of this complex is presented in Figure 3.

To assign the absolute chirality of **1**, the CD spectrum of the Λ enantiomer of **1a** was computed at the BP86 level accounting for the first 94 allowed UV/vis transitions. This range should adequately cover all of the MLCT and $\pi-\pi^*$ transitions affected by the chiral twist of the molecule, which would be minimally perturbed by the peripheral differences between **1** and **1a**, allowing direct comparison between theory and experiment at longer wavelengths. The simulated spectrum in Figure 1 was generated by first shifting all of the computed transitions to the blue by 0.65 eV (to correct for the underestimation of MLCT transitions at the TDBP86 level). Next, a Gaussian function was centered on each transition (eq 1)

$$g(\epsilon_\lambda;\alpha,R_0) = \frac{R_0}{22.97}\left(\frac{\alpha}{\pi}\right)^{1/2} \exp[-\alpha(\epsilon_\lambda - \epsilon_{\lambda_0})^2] \qquad (1)$$

where R_0 is the computed rotatory strength in units of 10^{-40} erg esu cm G^{-1} (length representation), α is chosen so that *g* has a width at half-maximum of 0.3 eV, ϵ_l is the energy in electronvolts corresponding to a given wavelength λ, and λ_0 is the wavelength of the shifted transition.[44] The simulated spectrum represents the sum of all 94 gaussians. It is apparent that the agreement between theory and experiment is quite good over the spectral range that is practical to access computation-

(32) Bauernschmitt, R.; Ahlrichs, R. *Chem. Phys. Lett.* **1996**, *256*, 454−464.
(33) Lee, C. T.; Yang, W. T.; Parr, R. G. *Phys. Rev. B* **1988**, *37*, 785−789.
(34) Becke, A. D. *J. Chem. Phys.* **1993**, *98*, 5648−5652.
(35) Stephens, P. J.; Devlin, F. J.; Chabalowski, C. F.; Frisch, M. J. *J. Phys. Chem.* **1994**, *98*, 11623−11627.
(36) Hehre, W. J.; Radom, L.; Schleyer, P. v. R.; Pople, J. A. *Ab Initio Molecular Orbital Theory;* Wiley: New York, 1986.
(37) Dolg, M.; Wedig, U.; Stoll, H.; Preuss, H. *J. Chem. Phys.* **1987**, *86*, 866−872.
(38) Frisch, M. J.; et al. *Gaussian 03*, revision B.05; Gaussian, Inc.: Pittsburgh, PA, 2003.
(39) Cramer, C. J. *Essentials of Computational Chemistry: Theories and Models*, 2nd ed.; Wiley & Sons: Chichester, 2004.
(40) Nitschke, J. R.; Schultz, D.; Bernardinelli, G.; Gérard, D. *J. Am. Chem. Soc.* **2004**, *126*, 16538−16543.
(41) Ameerunisha, S.; Schneider, J.; Meyer, T.; Zacharias, P. S.; Bill, E.; Henkel, G. *Chem. Commun.* **2000**, 2155−2156.
(42) Robin, M. B.; Day, P. *Adv. Inorg. Chem. Radiochem.* **1967**, *10*, 247−422.
(43) Jeffery, J. C.; Riis-Johannessen, T.; Anderson, C. J.; Adams, C. J.; Robinson, A.; Argent, S. P.; Ward, M. D.; Rice, C. R. *Inorg. Chem.* **2007**, *46*, 2417−2426.
(44) Pulm, F.; Schramm, J.; Hormes, J.; Grimme, S.; Peyerimhoff, S. D. *Chem. Phys.* **1997**, *224*, 143−155.

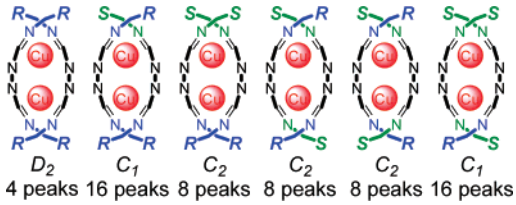

Figure 4. Six possible diastereomers of helicate **1** when racemic amine is used as a subcomponent. Only one enantiomer of each is shown. The point group and number of aromatic and imine ^{1}H NMR peaks expected for each diastereomer are given.

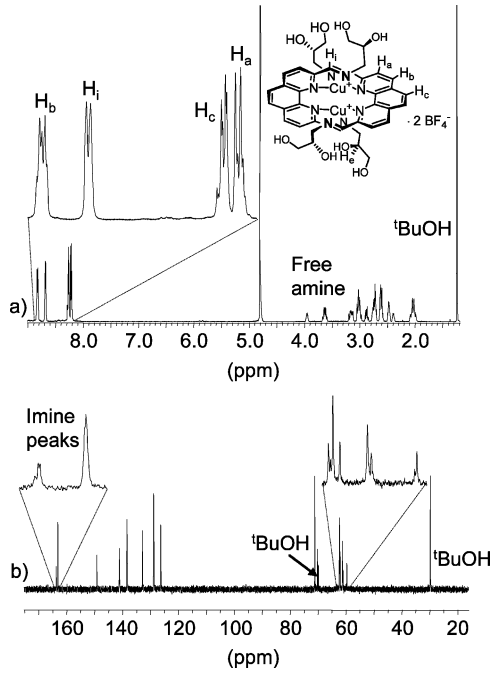

Figure 5. (a) 500 MHz ^{1}H and (b) 126 MHz ^{13}C NMR spectra of the mixture of diastereomers obtained in D_2O at 298 K when racemic aminopropanediol was used as a subcomponent in the reaction of Scheme 1.

ally[45] and unambiguously establishes the Λ enantiomer of **1** as the one isolated experimentally.

In principle, six diastereomeric pairs of enantiomers could be formed during the self-assembly process when racemic 1-amino-2,3-propanediol is used as a subcomponent. These are enumerated in Figure 4. Complex ^{1}H and ^{13}C NMR spectra (Figure 5) were obtained when this amine was used as a subcomponent, in keeping with the formation of a complex mixture of diastereomers that do not undergo rapid exchange on the NMR time scale. The CD spectrum of this mixture was featureless, as expected.

Since only the Λ helicate was observed when the *S* amine was used as a subcomponent (Scheme 1), we do not consider the 4*S*-Δ helicate or its enantiomer among the possibilities. Some degree of helical chirality induction might be expected in the 3*S*1*R* and 3*R*1*S* diastereomers as well. In the simplest case of perfect chiral induction (in which 3*S*1*R* gave only one product helicity), we would nonetheless expect the remaining mixture of diastereomers to give rise to 44 closely grouped aromatic and imine ^{1}H and ^{13}C NMR peaks. Because of the close peak spacing, we were not able to fully interpret the experimental NMR spectra. It is possible to state, however, that the spectra were consistent with the presence of numerous diastereomers and could not have come from two or fewer diastereomers.

When the preparation of helicate **1** and its diastereomers was carried out in methanol using racemic amine starting material, X-ray quality crystals were observed to form upon standing for two weeks at room temperature. Despite the complexity of the mixture of diastereomers present in solution, only **1** and its enantiomer were present in the crystal. Complex **1** shows crystallographic D_2 symmetry with the Cu atoms located in special positions 4*l* in the space group *Pban*. The crystal consists of distinct columns of Δ and Λ enantiomers in which the four equivalent hydroxyl groups link homochiral molecules together via hydrogen bonds (O···O = 2.742(4) Å). An ORTEP diagram of **1** is shown in Figure 6, along with views of the crystal packing. This structure indicated that the chiral amine residues of **1** induced the same helical chirality in the solid state as in solution, as indicated by the calculated CD spectrum (Figure 1).

When the reaction was run at a copper(I) concentration of 0.19 M in methanol, the isolated yield of crystalline product was 75%. Statistically, we would expect these two enantiomers to comprise 12.5% of the mixture; we found no evidence of extreme deviation from statistical self-assembly of diastereomers in methanol solution (see below). To rule out the possibility that our crystal was not representative of the bulk, three powder X-ray diffraction measurements taken on independently prepared samples of crystals were made. These measurements indicated that only a single phase was present (Figure 7) and matched the calculated powder diffraction pattern of the single crystal structure very well.

We concluded therefore that rearrangement occurred at the same time as the crystallization process: The dynamic combinatorial library[14] of diastereomers present in solution was sorted[46,47] during the crystallization process.

The lower solubility of **1** and its enantiomer in methanol may have been a consequence of their ability to form a crystalline network with four hydrogen bonds per molecule. The regularity of these linkages might be difficult to maintain between lower-symmetry diastereomers, leading them to stay in solution. Imine metathesis[15,16] and ligand exchange[48−54] appear thus to have allowed the diastereomers to interconvert in solution, funneling and sorting the subcomponents of the dynamic library into a mixture of **1** and its enantiomer, which were progressively removed from the mixture via crystallization.

Several different experimental observations suggested to us that the high degree of organization present in the crystals was

(45) A simulated spectrum at the TD B3LYP level shows improved agreement and does so with a much smaller peak offset, but for technical reasons it was not possible to extend this spectrum beyond the first 30 excitations, which fails to access the region of the spectrum to the blue of about 480 nm.

(46) Saur, I.; Scopelliti, R.; Severin, K. *Chem.−Eur. J.* **2006**, *12*, 1058−1066.
(47) Yang, H. B.; Ghosh, K.; Northrop, B. H.; Stang, P. J. *Org. Lett.* **2007**, *9*, 1561−1564.
(48) Severin, K. *Coord. Chem. Rev.* **2003**, *245*, 3−10.
(49) Elsevier, C. J.; Reedijk, J.; Walton, P. H.; Ward, M. D. *Dalton Trans.* **2003**, 1869−1880.
(50) Sun, W.-Y.; Yoshizawa, M.; Kusukawa, T.; Fujita, M. *Curr. Opin. Chem. Biol.* **2002**, *6*, 757−764.
(51) Seidel, S. R.; Stang, P. J. *Acc. Chem. Res.* **2002**, *35*, 972−983.
(52) Holliday, B. J.; Mirkin, C. A. *Angew. Chem., Int. Ed.* **2001**, *40*, 2022−2043.
(53) Albrecht, M. *Chem. Rev.* **2001**, *101*, 3457−3497.
(54) Caulder, D. L.; Raymond, K. N. *J. Chem. Soc., Dalton Trans.* **1999**, 1185−1200.

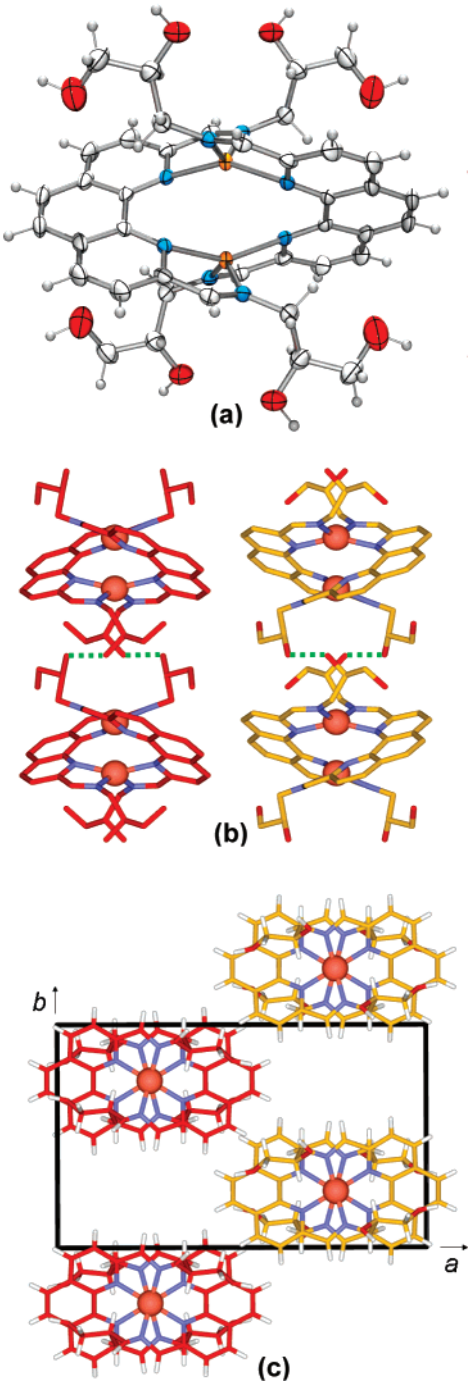

Figure 6. View of the crystal structure of **1** showing: (a) ORTEP view of 4*S*-Λ **1** along one of the three C_2 axes passing through the complex; Cu···Cu = 2.7410(7) Å; red ellipsoids correspond to oxygen atoms, gray to carbon, blue to nitrogen, orange to copper, and white spheres correspond to hydrogen; (b) the formation of columns, parallel to the [001] direction, of homochiral helicates (Λ and Δ enantiomers in red and yellow, respectively) linked by a network of hydrogen bonds; (c) the disposition of the columns in the unit cell viewed along the *c*-axis; the partially disordered BF_4^- anions present in the voids between helicates are not shown for clarity.

undone upon dissolution in two distinct, hierarchical[55] steps, as shown in Scheme 2. Initial, rapid ligand exchange appeared to produce the mixed-ligand diastereomer shown, and subsequent, slower imine exchange appeared to have regenerated the full set of diastereomers. These observations are discussed below.

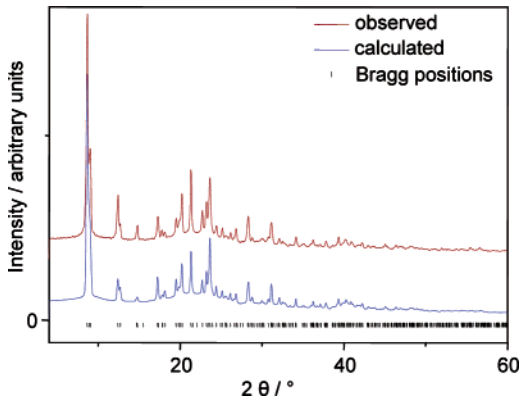

Figure 7. Observed (upper) X-ray powder pattern obtained from a bulk sample of **1**. The structural model of the calculated (lower) pattern corresponds to the crystal structure of **1** and its enantiomer obtained from single crystal measurement; the line width and shape were refined from the observed data. Positions of Bragg reflections are shown by ticks at the bottom.

Scheme 2. Proposed Two-Stage Ligand (Fast) and Imine (Slow) Exchange Following the Dissolution of Crystals of Racemic **1**

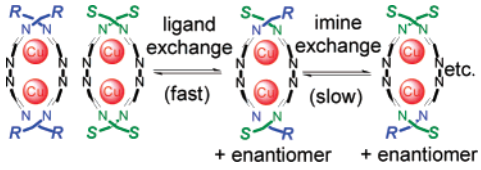

When the crystals containing **1** and its enantiomer were dissolved in water (4.8 mM), the resulting ^{1}H NMR spectrum was not the same as that of **1** (prepared from enantiopure amine), nor was it identical to the spectrum of the mixture of diastereomeric helicates from which the crystals had formed. The aromatic region of the ^{1}H NMR spectra of the dissolved crystals is shown in Figure 8a. Over the course of 4 days at room temperature, the spectrum of the dissolved crystals became indistinguishable from that of the original mixture of diastereomers. This was consistent with a slow imine exchange, but we were puzzled by our inability to observe the initial mixture of the two enantiomers of **1** before ligand exchange.

We suspected that the intimate mixing of both enantiomers in the dissolving crystal had resulted in a high concentration at the zone where dissolution occurred, leading to a ligand exchange too rapid to follow. To test this hypothesis, we mixed aqueous solutions of **1** and its enantiomer (both 2.4 mM), prepared separately from the two enantiomers of 1-amino-2,3-propanediol. In this case, ligand exchange took place slowly enough to be monitored by NMR; all observations indicated that both kinds of exchange occur slowly on the NMR time scale. An initial spectrum, taken 15 min after mixing, showed only a small shoulder adjacent to the imine peak (Figure 8b). Within 2 h at room temperature, the ^{1}H spectrum of this mixture was identical to that of the dissolved crystals; it subsequently became identical to that of the mixture of diastereomers over the same time frame as had the sample prepared from dissolved crystals.

These experiments were thus consistent with a rapid ligand exchange followed by a slower imine exchange, as shown in Scheme 2, but not vice versa. If imine exchange had occurred

(55) Albrecht, M.; Mirtschin, S.; de Groot, M.; Janser, I.; Runsink, J.; Raabe, G.; Kogej, M.; Schalley, C. A.; Froehlich, R. *J. Am. Chem. Soc.* **2005**, *127*, 10371−10387.

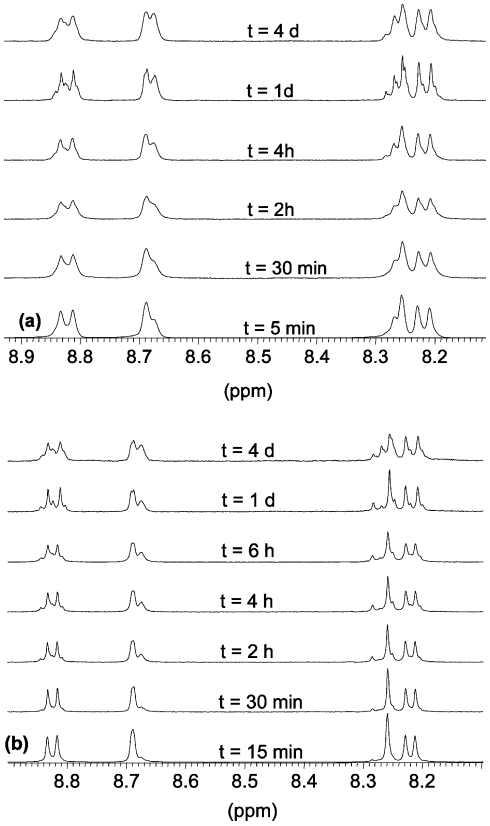

Figure 8. ^{1}H NMR spectra of (a) evolution with time of dissolved crystals of **1** and its enantiomer and (b) a 1:1 mixture of **1** and its enantiomer, dissolved separately (400 MHz, D_2O, 298 K).

more rapidly than ligand exchange, the full mixture of diastereomers would have been generated immediately. Ligand exchange would have been hidden by this process, since it adds only one diastereomer to the mixture.

Conclusions

Investigations of the expression of chiral information during self-organization have led to the development of a remarkable array of structures and functions,[17,19,56−60] from the sergeants-and-soldiers principle[61,62] to a light-powered rotor.[63,64] The chiral information expressed by the system comprising helicate **1** and its diastereomers allowed us to track separately the reversible ligand-exchange and imine-exchange processes occurring within this mixture of structures. The sorting of this dynamic library[14] during crystallization provided a novel example of the conversion of a complex mixture of diastereomers into a single pair of enantiomers, driven by the lower solubility of the latter. DFT calculations illuminated the nature of the MLCT transitions of this class of dicopper double helicates and also allowed us to determine that the chiral amine residues of **1** induced the same helical chirality in solution as in the solid state.

Future work will investigate the transfer of chiral information during subcomponent substitution. The displacement of the chiral amine residues from **1** via the addition of sulfanilic acid[40] produced a racemic complex. The use of a dianiline, however, might allow for the conservation of chiral information through the formation of a catenane.[65] In particular, substitution using an asymmetrical dianiline might allow the point chirality of the chiral amine residues to be translated through the helical chirality of a helicate into the persistent topological chirality[66] of a catenane.

Experimental Section

General. All manipulations were carried out in degassed solvents using reagents of the highest commercially available purity. $Cu(NCMe)_4BF_4$ was prepared following literature procedures.[67] NMR spectra were assigned with the help of COSY, ROESY, NOESY, HSQC, and HMBC measurements.[68] All chemical shifts were referenced to the residual proton or carbon signal of the solvent or to 2-methyl-2-propanol at $\delta = 1.24$ (^{1}H) or 30.29 (^{13}C) in D_2O as the internal standard. Repeated elemental analysis of **1** gave data within 0.7% of calculated values; boron-containing compounds often present analytical difficulties because of the formation of incombustible residues.[69]

Synthesis of Helicate 1. To a 50-mL Schlenk flask were added (*S*)-(−)-1-amino-2,3-propanediol (64.7 mg, 0.710 mmol, 2 equiv), 2,9-diformyl-1,10-phenanthroline[40] (84.0 mg, 0.355 mmol, 1 equiv), and water (5 mL). The flask was sealed, and the atmosphere was purified of dioxygen by three evacuation/argon fill cycles. Then, $Cu(NCMe)_4BF_4$ (111.7 mg, 0.355 mmol, 1 equiv) was added, immediately giving a green solution. The atmosphere was once more purified of dioxygen by three evacuation/argon fill cycles. The reaction was stirred at room temperature overnight. Volatiles were then removed under dynamic vacuum, giving an isolated yield of 177.8 mg (0.167 mmol, 94%) of microcrystalline green product. ^{1}H NMR (500 MHz, 298 K, D_2O): δ 8.85 (d, $J = 8$ Hz, 4H, 4,7-phenanthroline), 8.71 (s, 4H, imine), 8.28 (s, 4H, 5,6-phenanthroline), 8.24 (d, $J = 8$ Hz, 4H, 3,8-phenanthroline), 3.05 (dd, $J = 8$ Hz, $J' = 4$ Hz, 4H, C═NCH_2C*HOHCH_2), 2.75 (m, 4H, C═NCH_2C*HOHCH_2), 2.64 (m, 4H, C═NCH_2C*HOHCH_2), 2.50 (m, 4H, C═NCH_2C*HOHCH_2), 2.06 (d, $J = 13$ Hz, 4H, C═NCH_2C*HOHCH_2); ^{13}C NMR (125.77 MHz, 298 K, D_2O): δ 163.7, 149.7, 141.6, 139.9, 133.4, 129.4, 126.8, 71.7, 62.8, 61.7. ESI-MS: *m*/*z* 445.3 ($[L + Cu]^+$), 827.1 ($[2L + Cu]^+$), 977.1 ($[2L + 2Cu + BF_4]^+$); HRMS *m*/*z* Calcd for $C_{40}H_{44}N_8O_8Cu_2BF_4$: 977.1903; Found: 977.1900. Anal. Calcd for $C_{40}H_{44}B_2Cu_2F_8N_8O_8\cdot 5.2H_2O$: C, 41.44; H, 4.73; N, 9.67. Found: C, 41.47; H, 4.00; N, 9.09. UV/vis (degassed methanol; λ (nm), ϵ (M^{-1} cm^{-1})): 683, 2000; 304, 36 900; 259, 50 800; 228, 54 500; 201, 49 700; CD (degassed methanol, 293 K; λ (nm), $\Delta\epsilon$ (cm^2 $mmol^{-1}$)): 315, −198.2; 261, +123.6; 227, +61.0.

Synthesis of Crystalline 1 and Its Enantiomer. To a 10-mL Schlenk flask were added (±)-1-amino-2,3-propanediol (50.1 mg, 0.550 mmol, 2 equiv), 2,9-diformyl-1,10-phenanthroline (64.9 mg, 0.275 mmol, 1 equiv), $Cu(NCMe)_4BF_4$ (86.5 mg, 0.275 mmol, 1 equiv), and methanol (1.5 mL). The flask was sealed, and the atmosphere was

(56) Clayden, J.; Lund, A.; Vallverdu, L.; Helliwell, M. *Nature* **2004**, *431*, 966−971.
(57) Nakade, H.; Jordan, B. J.; Xu, H.; Han, G.; Srivastava, S.; Arvizo, R. R.; Cooke, G.; Rotello, V. M. *J. Am. Chem. Soc.* **2006**, *128*, 14924−14929.
(58) Dolain, C.; Jiang, H.; Leger, J. M.; Guionneau, P.; Huc, I. *J. Am. Chem. Soc.* **2005**, *127*, 12943−12951.
(59) Lam, R. T. S.; Belenguer, A.; Roberts, S. L.; Naumann, C.; Jarrosson, T.; Otto, S.; Sanders, J. K. M. *Science* **2005**, *308*, 667−669.
(60) Chambron, J.-C.; Dietrich-Buchecker, C.; Rapenne, G.; Sauvage, J.-P. *Chirality* **1998**, *10*, 125−133.
(61) Green, M. M.; Reidy, M. P.; Johnson, R. D.; Darling, G.; O'Leary, D. J.; Willson, G. *J. Am. Chem. Soc.* **1989**, *111*, 6452−6454.
(62) Palmans, A. R. A.; Vekemans, J.; Havinga, E. E.; Meijer, E. W. *Angew. Chem., Int. Ed.* **1997**, *36*, 2648−2651.
(63) Koumura, N.; Zijistra, R. W. J.; Van Delden, R. A.; Harada, N.; Feringa, B. L. *Nature* **1999**, *401*, 152−155.
(64) Eelkema, R.; Pollard, M. M.; Katsonis, N.; Vicario, J.; Broer, D. J.; Feringa, B. L. *J. Am. Chem. Soc.* **2006**, *128*, 14397−14407.
(65) Hutin, M.; Schalley, C. A.; Bernardinelli, G.; Nitschke, J. R. *Chem.−Eur. J.* **2006**, *12*, 4069−4079.
(66) *Molecular Catenanes, Rotaxanes and Knots: A Journey through the World of Molecular Topology;* Sauvage, J.-P., Dietrich-Buchecker, C., Eds.; Wiley-VCH: Weinheim, Germany, 1999.
(67) Ogura, T. *Transition Met. Chem. (Dordrecht, Neth.)* **1976**, *1*, 179−182.
(68) Braun, S.; Kalinowski, H.-O.; Berger, S. *150 and More Basic NMR Experiments: A Practical Course*, 2nd ed.; Wiley-VCH: Weinheim, Germany, 1998.
(69) James, T. D.; Sandanayake, K. R. A. S.; Shinkai, S. *Angew. Chem., Int. Ed.* **1996**, *35*, 1911−1922.

purified of dioxygen by three evacuation/argon fill cycles, giving a green solution. The solution was heated at 50 °C overnight and kept at room temperature during two weeks. The supernatant was then removed with a syringe and kept under an argon atmosphere; it deposited no crystals during 5 days. The green crystalline powder was dried under vacuum, giving an isolated yield of 109.5 mg (74.7%).

Crystallographic Data for 1 and Its Enantiomer: $[Cu_2(C_{20}H_{22}N_4O_4)_2](BF_4)_2$; $M_r = 2172.3$, orthorhombic, *Pban*, $a = 19.4766(10)$, $b = 11.8014(5)$, $c = 9.9226(6)$ Å, $V = 2280.7(2)$ Å^3; $Z = 2$, $\mu = 1.025$ mm^{-1}, $d_x = 1.552$ g cm^{-3}, Mo Kα radiation ($\lambda = 0.71073$ Å); 31 592 reflections measured at 200 K, 2473 unique reflections of which 1412 were observables ($|F_o| > 4\sigma(F_o)$). Data were corrected for Lorentz and polarization effects and for absorption (T_{min}, $T_{max} = 0.7759$, 0.9593). The structure was solved by direct methods (SIR97).[70] All calculations were performed with the XTAL system.[71] Full-matrix least-squares refinement based on F using weights of $1/(\sigma^2 (F_o) + 0.00015(F_o^2))$ gave final values $R = \omega R = 0.037$, and $S = 1.84(4)$ for 176 variables and 1516 contributing reflections. Powder patterns were obtained on a Stoe Stadi-P powder diffractometer with Cu Kα$_1$ radiation ($\lambda = 1.54059$ Å), curved image plate detector, sample in a 0.5-mm glass capillary and exposure time of 4 h.

Acknowledgment. This work was supported by the U.S. National Science Foundation (CHE-0610183) and the Swiss National Science Foundation (200021-111645 and 20EC21-112708). We thank H. Flack for critical comments on the manuscript, P. Perrottet for mass spectrometric analyses, A. Pinto for ROESY NMR spectra, and D. Jeannerat for help in interpreting the NMR spectra.

Supporting Information Available: Complete ref 38, ^{1}H and ^{13}C NMR spectra of **1** and the mixture of its diastereomers. Full structural details for the crystal structure of **1** and its enantiomer (CIF). This material is available free of charge via the Internet at http://pubs.acs.org. Full structural details have also been deposited as CCDC-626728. These data can be obtained free of charge via www.ccdc.cam.ac.uk/conts/retrieving.html (or from the Cambridge Crystallographic Data Centre, 12 Union Road, Cambridge CB2 1EZ, U.K.; fax: (+44) 1223−336-033; or deposit@ccdc.cam.ac.uk).

JA070320J

(70) Altomare, A.; Burla, M. C.; Camalli, M.; Cascarano, G.; Giacovazzo, C.; Guagliardi, A.; Moliterni, A. G. G.; Polidori, G.; Spagna, R. *J. Appl. Crystallogr.* **1999**, *32*, 115−119.
(71) Hall, S. R.; Flack, H. D.; Stewart, J. M. *Xtal 3.2 User's Manual;* University of Western Australia: Perth, Australia, 1992.